Processing and Application of Ceramics 10 [2] (2016) 87–95
DOI: 10.2298/PAC1602087M

Glass-like carbon, pyrolytic graphite or nanostructured carbon for electrochemical sensing of bismuth ion?

Jadranka Milikić, Nevena Markičević, Aleksandar Jović, Radmila Hercigonja, Biljana Šljukić*

Faculty of Physical Chemistry, University of Belgrade, Studentski trg 12–16, 11158 Belgrade, Serbia

Received 29 April 2016; Received in revised form 16 June 2016; Accepted 20 June 2016

Abstract

Different carbon electrodes were explored for application in electroanalysis, namely for sensing of bismuth ion as model analyte. Carbon materials tested included glassy carbon, basal and edge plane pyrolytic graphite, as well as nanostructured carbonized polyaniline prepared in the presence of 3,5-dinitrosalicylic acid. Bismuth ion was chosen as model analyte as protocol for its detection and quantifications is still to be determined. Herein, anodic stripping voltammetry was used with study of effect of several parameters such as scan rate and deposition time. Electrode based on carbonized polyaniline showed the highest activity for bismuth ion sensing in terms of the highest current densities recorded both in a laboratory and in real sample, while basal plane pyrolytic graphite electrode gave the lowest limit of detection.

Keywords: *bismuth, basal plane pyrolytic graphite, edge plane pyrolytic graphite, glassy carbon, carbonized polyaniline, anodic stripping voltammetry*

I. Introduction

The environment is constantly polluted by heavy metals' emissions from numerous industrial processes and their accumulation in nature [1–5]. Depending on chemical forms and concentrations, heavy metals can pose a hazard to people and to the environment. Many heavy metals' salts are soluble in water and cannot be removed by the usual physical processes. Thus, these pollutants are continuously concentrated in the environment [6,7].

Bismuth and its salts can cause damage to the kidneys, liver and bladder, and larger doses can be lethal. Bismuth in the human body can also cause irritation of the respiratory system and skin. Bismuth could be introduced into human body by inhalation, ingestion or through the skin. The influence of bismuth on the environment has not been fully tested yet. Because of its poor solubility, it is considered that bismuth is less harmful for the environment than other heavy metals. However, this metal should be especially carefully observed, because of limited information on its effects on the environment [8].

In line with this, it is necessary to develop sensitive, effective and efficient methods for detection of heavy metal ions in aqueous solution, as well as methods for their removal. Electrochemical sensors are very attractive and suitable for heavy metal ions sensing due to their simple use, fast and highly selective response to the analyte, with often no pretreatment necessary for analysis of complex samples. Thanks to a wide potential range in which they can be used, high heat resistance and chemical inertness, as well as low price, carbon electrodes are very often used in electroanalytical purposes [9–13]. However, the transfer of electrons at carbon electrodes is often slow and requires a high overvoltage for oxidation or reduction process. Recently, application of different nanostructured carbon materials in electroanalysis has been suggested. Special attention in the latest researches is given to nitrogen-containing nanostructured carbons (NNCs) employment in sensor and biosensor [14,15]. Among different NNCs, polyaniline (PANI), nanostructured N-containing conducting polymer, stands out for its simple synthesis method with easily controlled morphology [16–19]. Nanostructured carbonized PANIs (c-PANI) showed excellent properties as electrocatalysts for different applications [20–24]. Using c-PANI based electrode for sensors and biosensors has also been recently reported [25–30]. Suc-

* Corresponding author: tel: +381 11 3336894,
fax: +381 11 2187133, e-mail: *biljka@ffh.bg.ac.rs*

cessful application of c-PANIs both as electrocatalysts support and as electrode materials for sensing of heavy metal ions has been demonstrated in our previous work [31,32].

The present paper examines the possibility of using carbon electrodes, namely, edge plane pyrolytic graphite (EPPG), basal plane pyrolytic graphite (BPPG), glassy carbon (GC) and GC electrode modified with c-PANI for electrochemical determination of bismuth ions by anodic stripping voltammetry with the aim to achieve low detection limits and high sensitivity.

II. Experimental procedures

All chemicals used in this work were of analytical grade and used as received from the manufacturer without further purification. All solutions were prepared using distilled water.

All electrochemical measurements were carried out on Gamry PCI4/300 Potentiostat/Galvanostat with a three-electrode glass cell of 15 cm^3 volume. Working electrodes used were BPPG, EPPG, GC (5 mm diameter, Pine Research Instrumentation), as well as GC modified with carbonized polyaniline prepared in the presence of 3,5-dinitriosalicylic acid (c-PANI-DNSA). BPPG and EPPG electrodes were prepared in house by mounting BPPG or EPPG disk of 5 mm diameter in Teflon. c-PANI-DNSA/GCE was prepared by pipetting 10 μl of catalytic ink onto clean and polished GCE, followed by drying at room temperature overnight. Catalytic ink was prepared by mixing c-PANI-DNSA (5 mg), nafion (50 μl) and ethanol (750 μl) and it was left to homogenise in ultrasonic bath for 30 min. Platinum and saturated calomel electrode (SCE) served as counter and reference electrode, respectively. All potentials in this work are given versus SCE. KCl–HCl buffer of pH 1.0 was prepared by mixing 0.2 M KCl solution (50 cm^3) and 0.2 M HCl solution (134 cm^3), and this buffer solution served as supporting electrolyte. All measurements were performed at room temperature.

Carbonized polyaniline was prepared by the gram-scale template-free oxidative polymerisation of aniline with ammonium peroxydisulfate as an oxidant in an aqueous solution of 3,5-dinitrosalicylic acid and subsequent carbonization of produced PANI [33,34].

Anodic striping voltammetry (ASV) was used for determination of bismuth, employing different scan rates and different deposition times with stirring during the deposition step.

III. Results and discussion

In the search for convenient method and electrode materials for qualitative and quantitative sensing in aqueous solution, sensing of bismuth by anodic stripping voltammetry in KCl–HCl buffer was herein explored. As potential electrode materials for bismuth sensing, four carbon electrodes were tested, namely BPPG, EPPG, GC and c-PANI-DNSA. GC and two orientations of pyrolytic graphite (basal and edge) were selected as the major carbon materials used in electrochemistry, while c-PANI-DNSA was selected as material that has been pointed out recently as suitable for electroanalytical applications.

Carbon materials' electrochemical response is governed by their microstructure, electronic structure, i.e. density of electronic states (DOS), hydrophobicity/hydrophilicity, surface cleanliness, as well as presence of surface oxides [13,29,35]. Pyrolytic graphite (PG) and GC have some common characteristics such as low gas permeability, high chemical inertness and electrical conductivity. Still, these carbon materials have different structures so that PG has polycrystalline sp^2 carbon structure that comprises edge-plane (EP, irregular surfaces perpendicular to graphite layers) and basal-plane pyrolytic graphite (BPPG, atomically ordered hexagonal planes parallel to graphite layers). Field emission scanning electron microscopy (FE-SEM) analysis of BPPG and EPPG surfaces revealed different morphologies so that basal plane is non-smooth, rough as compared to edge plane at which edges of layers could be clearly distinguished [36]. Atomic force microscopy (AFM) analysis revealed that BPPG still contains some step edges whose density depends on the electrode's history and preparation, while EPPG also contains some basal planes but the terraces are very short compared to those at BPPG [37]. GC is considered to be an advanced pure carbon material combining glassy and ceramic

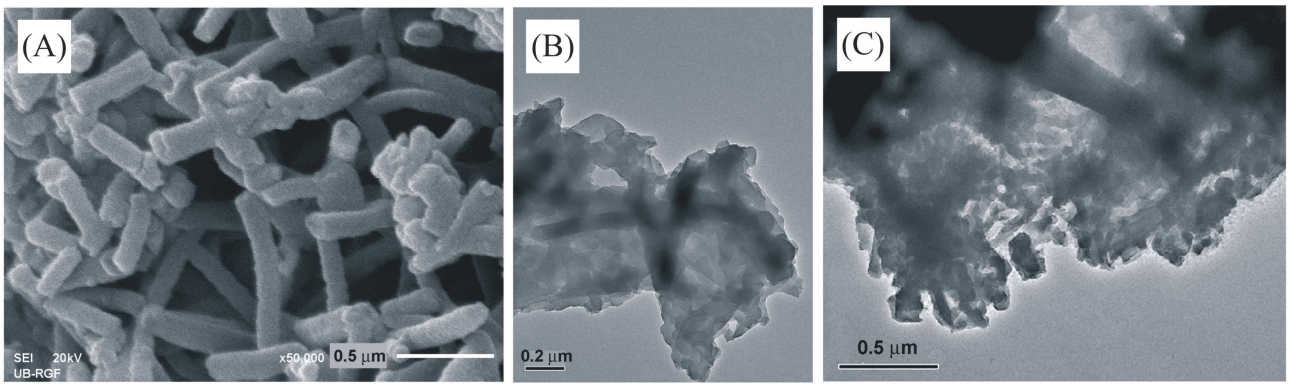

Figure 1. SEM (A) and TEM (B and C) images of c-PANI-DNSA (adapted from [29] with permission from Elsevier)

properties with those of graphite. Contrasting graphite, GC has a fullerene-related microstructure comprising highly disordered and randomly intertwined ribbons of graphitic planes forming mixture of sp^2 and sp^3 carbon domains. AFM and FE-SEM analysis of GC surface showed that it is a flat, smooth, non-porous surface with low roughness factor [38]. Morphology of c-PANI-DNSA was studied by SEM and TEM that revealed that c-PANI-DNSA predominantly consists of nanorods, with some edge-plane like sites, Fig. 1 [29].

Raman spectra of perfect graphite have two bands, at 47 cm^{-1} and at 1582 cm^{-1} (G, graphite band) and two infrared bands at 868 and 1588 cm^{-1} [42,43]. Raman spectra of GC contain additional band at ca. 1360 cm^{-1} (D, disorder band) with broaden G band of slightly higher frequency [41]. Raman spectra of c-PANI-DNSA contain both G and D band at 1354 and 1590 cm^{-1}, respectively, with I_D/I_G ratio of 3.68, and infrared bands at 1260 and 1553 cm^{-1} [29,33]. Presence of D band with $I_D/I_G > 1$ and broadening of bands is characteristic for disordered graphite with reduced crystallite size.

Carbon materials studied herein have different electrical conductivity. PG is anisotropic so that resistance parallel to graphite layers is much lower than perpendicular to the layers. Resistivity of GC is reported to be of 10^{-3} Ω cm order [41]. Electrical conductivity of c-PANI-DNSA is reported to be ca. 0.35 S cm [29,33].

Furthermore, density of electronic states differs considerably for different carbon materials studied herein. DOS determines heterogeneous rate constant with higher DOS meaning higher probability that an electron of the right energy is available for electron transfer to a redox system. Graphite is semimetallic with DOS at the Fermi level of ca. $(2–6)\times10^{20}$ $cm^{-3}\cdot eV^{-1}$, for potentials and conditions relevant to aqueous electrochemistry [39,40]. On the other hand, GC is considered to possess a DOS comparable to that of metal electrodes, such as gold [41].

Carbon materials studied also have different surface chemistry that is generally significantly more complex than for metals. Namely, majority of carbon surfaces react with oxygen and water so that oxygen-containing functional groups (carbonyls, phenolic OH, lactones, ethers and carboxylates) are present on those surfaces unless special pre-treatments are carried out. Thus, unlike BPPG, EPPG and, especially, GC surface are rich in oxygen-containing moieties [41]. Surface oxygen functional groups, specifically phenol, ether and carboxyl groups were identified by XPS analysis of c-PANI-DNSA, while no quinone type groups were present [29,33]. The negative surface charge due to carboxylates presence can substantially influence ionic analytes adsorption and electron transfer rates [41]. The magnitude of interactions between surface and adsorbate, dipole-dipole interactions, induced dipoles, hydrophobic effects, and electrostatic and covalent bonds, is determined by the type of carbon material, its history and preparation, i.e., its surface chemistry, exposure of basal or edge planes at the surface, and the distribution of surface oxides. Polar surface carbon-oxygen groups lead to strong dipole-dipole or ion-dipole interactions that promote adsorption [44]. Accordingly, adsorption on the basal plane is expected to be relatively weak, since there are no permanent dipoles, electrostatic charges, or unsatisfied valences. Conversely, adsorption is expected to be strong on edge plane graphite and on step-edge defects on the basal plane [41].

Having in mind influence of electrode's history on its electrochemical performance, all electrodes were pretreated prior to the measurements [13,35]. Different pretreatment procedures were applied depending on the electrode used. Thus, GCE surface was polished with diamond paste and, after careful rinsing with water, it was sonicated in HNO_3 solution for 10 min. EPPG electrode surface was polished to a mirror-like finish with alumina slurry, followed by thorough rinsing with water removing any alumina residue. BPPG electrode surface was first polished on carborundum paper and then cellotape was pressed on the clean electrode surface and removed along with several surface layers of graphite. BPPG electrode was finally cleaned in acetone to remove any adhesive residue.

Possible application of BPPG electrode for bismuth sensing was first studied by recording ASV in KCl–HCl buffer in the potential range from −0.45 to 0.35 V at a scan rate of 50 mV/s and with deposition time of 60 s during which electrode was held at potential of −0.45 V and solution was stirred. Control voltammogram recorded in buffer solution with no bismuth present exhibited no peaks. Subsequently, bismuth stock solution was added to the buffer to build up 10 μM bismuth solution and voltammogram was recorded again under the same conditions as in the case of buffer. At the ASV recorded, two clear peaks are seen, at −0.07 and 0.17 V, corresponding to the oxidation of metal bismuth deposited on the electrode surface during the deposition step. Appearance of two peaks suggests that bismuth oxidation proceeds at different planes of BPPG electrode.

Next, bismuth concentration increased in the 10–100 μM range using 10 μM step and ASV of BPPG was recorded for each concentration, Fig. 2A. Currents of oxidation peak at ca. −0.07 V were used for construction of standard addition plot of peak current versus bismuth concentration. Linear increase of peak current with increasing concentration could be observed in the studied concentration range. Using data from this graph, *LOD* of bismuth ion with BPPG electrode was evaluated using 3 sigma method [45]:

$$LOD = 3\sigma/b \quad (1)$$

where σ is the standard deviation of the y-coordinate from the line of best fit and b the slope of the same line. *LOD* of bismuth ion determination in aqueous solutions using ASV with BPPG electrode was calculated to be 2.6 μM, while the sensitivity was found to be 5.9 A/M.

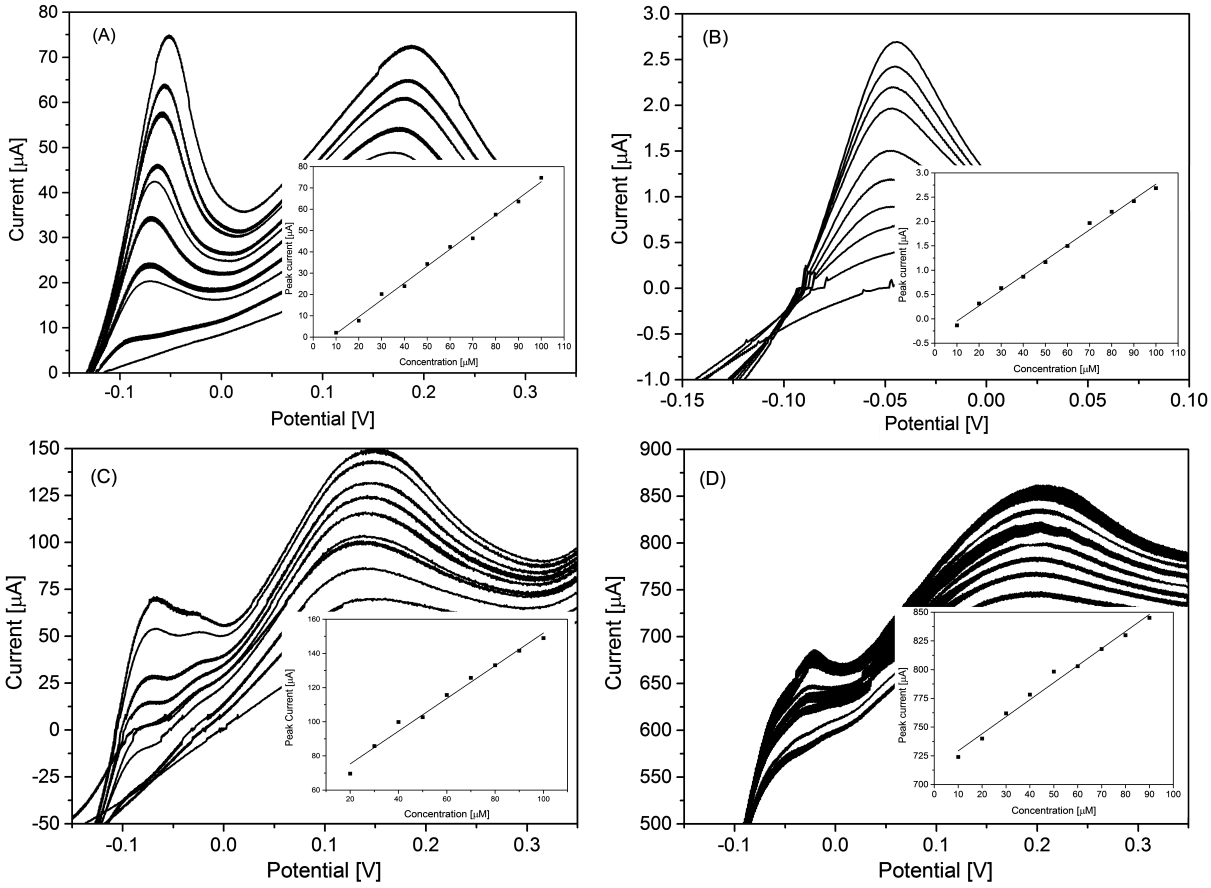

Figure 2. Increase of BPPG (A), EPPG (B), GC (C) and c-PANI-DNSA (D) electrode voltammetric signal with increase of bismuth concentration in the 10–110 μM range

Next, voltammograms of EPPG electrode were recorded under the same experimental condition as in the case of BPPG electrode, with bismuth oxidation giving a single well-defined peak at ca. −0.05 V. Comparison of voltammograms of BPPG and EPPG electrodes in bismuth solution reveals two distinctive differences — absence of the second oxidation peak at 0.17 V and notably smaller anodic currents in case of EPPG. For instance, BPPG electrode gave a peak current of 77 μA, while EPPG electrode gave peak current of only 2.7 μM in 100 μM bismuth solution in KCl–HCl buffer. BPPG and EPPG electrodes are known to give different electrochemical response due to mentioned major differences in properties such as surface morphology and chemistry, as well as resistance [36,41]. Electron transfer at BPPG electrode has been reported to be up to 10^3 times slower compared to EPPG electrode, resulting in higher overpotentials needed for oxidation/reduction process [41,46]. Thus, better electroanalytical response of EPPG electrode with faster electrode kinetics compared to BPPG (as well as some other carbon) electrode has been reported for different analytes [47–54]. However, recent reports say that BPPG and EPPG electrode can give similar response for sensing of compounds such as dopamine and epinephrine by electrooxidation [37,55,56]. Moreover, better electroanalytical response of BPPG compared to EPPG electrode has been reported for instance for sensing of oxalates in aqueous solutions [13]. Possibility of fast electron transfer and electrochemical activity of BP was further confirmed by recent studies of diffusion process [57] as well as of metal nanoparticle electrodeposition process on edge planes and basal planes of highly oriented pyrolytic graphite (HOPG). These studies showed that density of step edge sites did not influence electrodeposition process (i.e. edge plane sites do not play a dominant role) and showed fast electron transfer at basal planes [58]. Additional confirmation was obtained from the latest studies of outer-sphere redox processes at HOPG and metals indicating that DOS does not play key role in the electron transfer kinetics of these processes at studied electrodes [59]. Namely, electron transfer kinetics was found to be fast at HOPG electrodes with different step edge sites density. It is believed that electrode's electronic structure stops playing important role in the electron transfer kinetics when there is strong electronic coupling between the redox couple and electrode because DOS of the studied electrodes (HOPG and metals) has orders of magnitude higher than those of the redox species in solution. Furthermore, it was suggested that the reactions could be even faster at HOPG than at metals such as Pt in some cases, due to the secondary effects, including double layer effects, nature of the metal and electrolyte on the Helmholtz layer.

Since EPPG electrode gave clear signal corresponding to bismuth oxidation, *LOD* of bismuth ion sensing in aqueous solutions using ASV with EPPG electrode was next determined. 10 μM bismuth additions were made to the supporting electrolyte up to the concentration of 100 μM and ASV run for each concentration. All ASVs gave a well-defined peak assigned to bismuth oxidation at ca. −0.05 V with peak current increasing linearly with the increase of concentration, Fig. 2B. Using 3 sigma method, *LOD* was evaluated to be 5.0 μM, while sensitivity was evaluated to be 0.03 A/M. *LOD* of bismuth ion sensing with EPPG was of the same order of magnitude as *LOD* with BPPG electrode and low enough to offer possibility of using EPPG electrode for bismuth ion sensing in aqueous solutions. Furthermore, sensitivity obtained with EPPG electrode was improved compared to that of BPPG electrode.

Next carbon material tested for qualitative and quantitative analysis of bismuth ions in aqueous solutions was GC with test conditions being the same as in the case of BPPG and EPPG electrodes. ASV recorded in the supporting electrolyte with no bismuth present showed no peaks. Subsequently, bismuth additions in the 10–100 μM range with 10 μM step were made and ASV recorded for each concentration, Fig. 2C. Similar to BPPG electrode, GCE gave two peaks corresponding to bismuth oxidation, a smaller one at ca. −0.07 V and a well-defined peak at ca. 0.17 V. Thus, bismuth oxidation peak potentials were practically the same in case of GCE and BPPG electrodes, while peak currents recorded with GCE were higher than in the case of BPPG and significantly higher than in the case of EPPG electrode. This is in agreement with previous reports on GC rates 1–3 orders of magnitude higher than those for PG for different redox systems, as a consequence of semimetal character of PG [60].

The appearance of clear peaks corresponding to bismuth oxidation at GCE indicated possibility of GCE application for electrochemical sensors for bismuth sensing in aqueous solution. In order to examine the possibility of quantitative determination of bismuth ion with GCE, currents corresponding to peak at 0.17 V recorded in solutions of different electrolytes were used to construct standard addition plot. Using 3 sigma method, *LOD* of bismuth ions sensing using ASV with GCE was evaluated to be 9.2 μM, which was somewhat higher than in the case of BPPG and EPPG electrode.

The last carbon material investigated for bismuth ions sensing in aqueous solutions was c-PANI-DNSA. Again, at ASV run in supporting electrolyte no peaks were seen. Conversely, two peaks could be seen at ASVs run in bismuth solutions of 10–110 μM concentration, a smaller peak at ca. −0.02 V and a bigger one at ca. 0.21 V, Fig. 2D. The peak currents were found to be considerably higher than those recorded at EPPG, BPPG and GC electrodes, most likely due to high specific surface area of this material (441 m^2/g) and porosity (mesopore surface area of 21 m^2/g and specific surface area of

Table 1. Comparison of bismuth ion sensing parameters at four carbon electrodes (peak current and peak potential values refer to 100 μM bismuth solution)

Electrode	BPPG	EPPG	GC	c-PANI-DNSA
I_p [μA]	77.0	2.7	148.0	850.0
E_p [V]	−0.07	−0.05	0.17	0.21
LOD [μM]	2.6	5.0	9.2	7.6

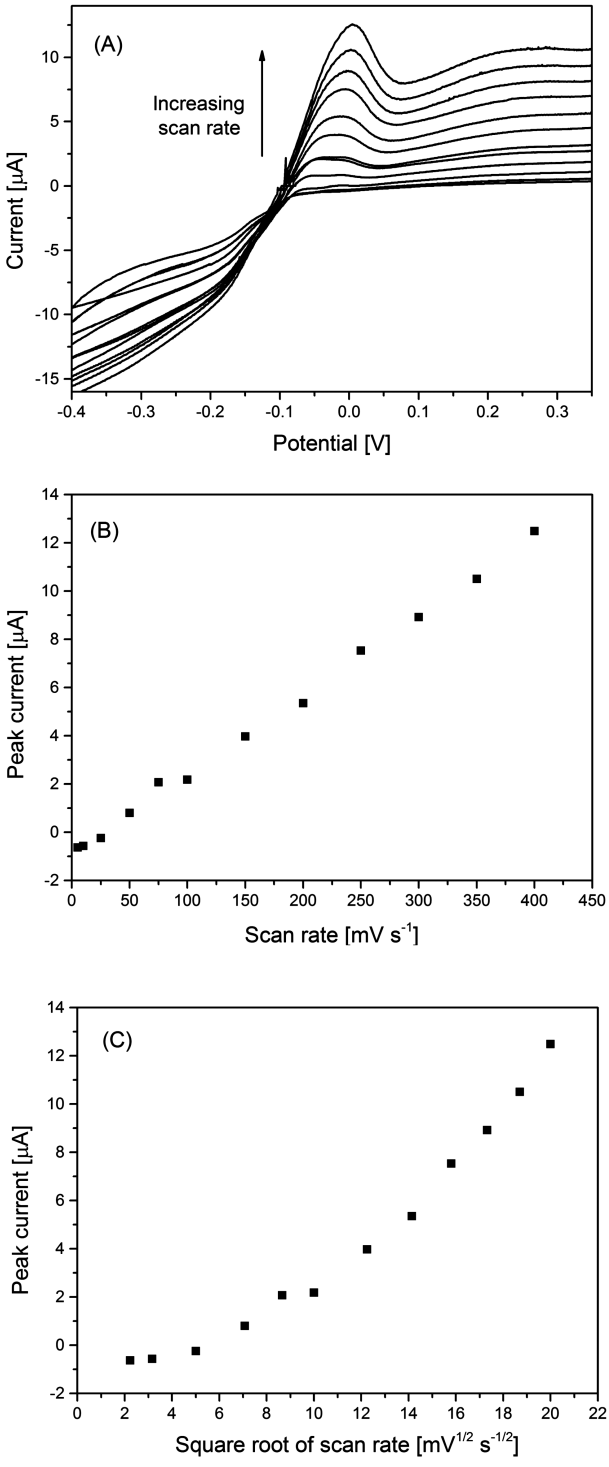

Figure 3. Increase of EPPG electrode voltammetric signal in 110 μM bismuth solution with increase of scan rate in 5–400 mV/s range

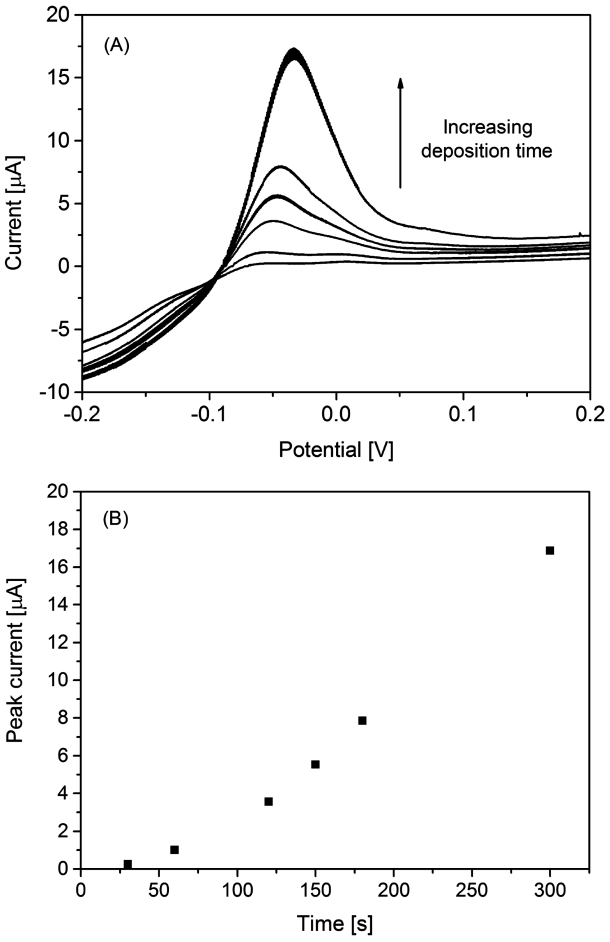

Figure 4. Increase of EPPG electrode voltammetric signal in 110 μM bismuth solution with increase of deposition time in 30–300 s range

micropores of 520 m^2/g) [29,34]. Namely, accessibility of the analyte is another important factors determining electrodes response and the accessibility is dependent on the pore structure and specific surface area of electrode material. Large specific surface area of c-PANI-DNSA enables better accessibility of analyte compared to other three herein studied carbon electrodes. Next, current of oxidation peak at 0.21 V was used for construction of peak current versus concentration plot resulting in a straight line. Using 3 sigma method, *LOD* of bismuth ions sensing in aqueous solutions using ASV with c-PANI-DNSA electrode was determined to be 7.6 μM. The obtained *LOD* value is somewhat lower than value obtained with GCE, but somewhat higher than values obtained with BPPG and EPPG electrode.

Table 1 summarises parameters of bismuth sensing in aqueous solutions using ASV with four studied carbon electrodes, namely peak potential, peak current and *LOD*. The highest peak currents were recorded at c-PANI-DNSA-based electrode, most likely due to the mentioned high specific surface area of this material. BPPG electrode exhibited the best performance in terms of the lowest *LOD*, though all *LOD*s determined had the same order of magnitude.

Next, electrooxidation of bismuth at EPPG electrode was investigated in more detail. The effect of the scan rate on the electrooxidation of bismuth at EPPG electrode was subsequently studied. ASVs of EPPG electrode were run in 110 μM bismuth solution using constant deposition potential of −0.45 V and constant deposition time of 60 s at scan rates ranging from 5 to 400 mV/s. The current responses of bismuth oxidation at EPPG electrode were presented as a function of scan rate and as a function of square root of scan rate, Fig. 3.

Linear dependence in first case is indicative of surface-confined species, while linear dependence in the second case is indicative of diffusion-control process. Peak current corresponding to bismuth oxidation increased in a straight line with scan rate in the studied range of 5–400 mV/s, confirming presence of surface-confined species, i.e. that anodic peak originates from oxidation of bismuth deposited on the electrode surface.

Subsequently, the influence of deposition time on the carbon electrodes response to bismuth was explored. ASVs of EPPG electrode were recorded in bismuth solution of constant concentration of 110 μM using a constant scan rate of 50 mV/s. Deposition potential of −0.45 V was kept constant throughout the measurements, while deposition times employed ranged from 30 to 300 s. Within the studied range, bismuth oxidation peak current was observed to practically exponentially increase with increase of deposition time, Fig. 4, thus indicating that further optimisation of bismuth ion sensing using ASV with carbon electrodes is possible.

Finally, the possibility of using ASV with carbon electrodes for analysis of bismuth ion in real samples was explored. ASVs of EPPG electrode were recorded at scan rate of 50 mV/s using 60 s deposition time. No peaks could be observed in control voltammogram recorded in tap water with no bismuth present in the sample. However, upon addition of 2.5 ml of bismuth stock solution in tap water, a peak corresponding to bismuth oxidation appeared at ca. −0.05 V, Fig. 5. Furthermore, BPPG, GC and c-PANI-DNSA-based electrode all gave clear signal to bismuth ion presence in tap water with oxidation peak current increasing in the follow-

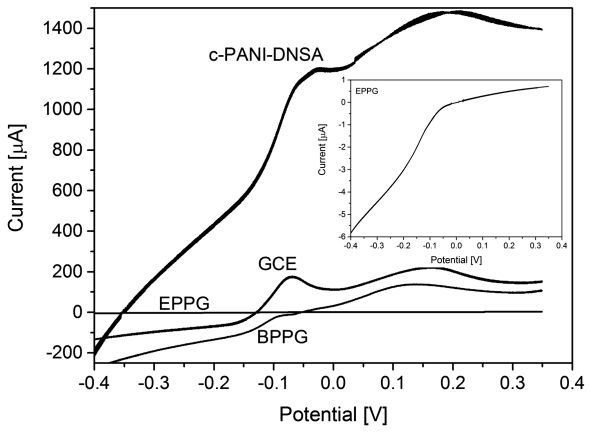

Figure 5. ASV response of four carbon electrode to bismuth presence in tap water

ing order c-PANI-DNSA > BPPG > GC > EPPG. It is worth noting that bismuth oxidation signal was recorded with no pre-treatment of the real sample.

IV. Conclusions

The activity of four different carbon electrodes, namely BPPG, EPPG, GC and c-PANI-DNSA electrode, for the determination of bismuth ions in aqueous solutions has been explored. Anodic stripping voltammetry was used and influence of parameters such as deposition time and scan rate was studied. Characteristic peaks corresponding to bismuth oxidation were recorded at all four electrodes, thus suggesting their potential application in electrochemical sensors for bismuth ions sensing. Peak current increased in the following order: EPGG < BPPG < GCE < c-PANI-DNSA. The highest peak current recorded at c-PANI-DNSA is most likely due to its high specific surface area and its porosity that allows better accessibility of analyte compared to other three herein studied electrodes. The BPPG electrode showed the best behaviour in terms of the lowest *LOD* as *LOD* increased in the following order: BPPG < EPGG < c-PANI-DNSA < GCE. The results obtained contribute to the latest findings on the intrinsic electroactivity of BPPG, evidencing that it can provide fast-rate electron transfer for various electrochemical processes. BPPG electroactivity is explained by relatively insignificant effect of DOS on electron transfer for electrodes studied herein. Moreover, the method was applied for sensing of bismuth ions in tap water and a clear response to bismuth presence was recorded. Thus, a simple and rapid method with inexpensive materials could be employed for bismuth ions analysis.

Acknowledgements: The authors would like to thank the Ministry of Education, Science and Technological Development of Republic of Serbia for support within the project No. OI172043 and OI172018. The authors would also like to thank professor Gordana Ćirić-Marjanović and ass. professor Aleksandra Janošević Ležaić for synthesis of carbonized polyaniline used in this work.

References

1. G. Wildgoose, H. Leventis, A. Simm, J. Jones, R. Compton, "Cysteine methyl ester modified glassy carbon spheres for removal of toxic heavy metals from aqueous media", *Chem. Commun.*, **29** (2005) 3694–3696.
2. C. Locatelli, "Heavy metals in matrices of food interest: Sequential voltammetric determination at trace and ultratrace level of copper, lead, cadmium, zinc, arsenic, selenium, manganese and iron in meals", *Electroanalysis*, **16** [18] (2004) 1478–1486.
3. U. Forstner, G.T.W. Wittmann, *Metal Pollution in Aquatic Environment*, Springer-Verlag, New York, 1981.
4. Y.X. Chen, H. Liu, G.W. Zhu, H.L. Chen, G.M. Tian, "Pollution characteristics of the recent sediments in the Hangzhou section of the Grand Canal, China", *J. Environ. Sci.*, **16** [1] (2004) 34–39.
5. A. Ahmad, M. Alam, "Sequestration and remediation of heavy metals by Brassica sp at Hindan river sites", *Indian J. Chem. Technol.*, **11** [4] (2004) 555–559.
6. J.P. Vernet, *Impact of Heavy Metals on the Environment*, Elsevier, New York, 1992.
7. M.P. Ireland, *Biological Monitoring of Heavy Metals*, Wiley, New York, 1991.
8. M. Vasić, B. Šljukić, G.G. Wildgoose, R.G. Compton, "Adsorption of bismuth ions on graphite chemically modified with gallic acid", *Phys. Chem. Chem. Phys.*, **14** [28] (2012) 10027–10031.
9. G.G. Wildgoose, P. Abiman, R.G. Compton, "Characterising chemical functionality on carbon surfaces", *J. Mater. Chem.*, **19** [28] (2009) 4875–4886.
10. A.C. Thorogood, G.G. Wildgoose, J.H. Jones, R.G. Compton, "Identifying quinone-like species on the surface of graphitic carbon and multi-walled carbon nanotubes using reactions with 2,4-dinitrophenylhydrazine to provide a voltammetric fingerprint", *New J. Chem.*, **31** (2007) 958–965.
11. A.C. Thorogood, G.G. Wildgoose, A. Crossley, R.M.J. Jacobs, J.H. Jones, R.G. Compton, "Differentiating between ortho- and para-quinone surface groups on graphite, glassy carbon, and carbon nanotubes using organic and inorganic voltammetric and X-ray photoelectron spectroscopy labels", *Chem. Mater.*, **19** (2007) 4964–4974.
12. A.T. Masheter, L. Xiao, G.G. Wildgoose, A. Crossley, J.H. Jones, R.G. Compton, "Voltammetric and X-ray photoelectron spectroscopic fingerprinting of carboxylic acid groups on the surface of carbon nanotubes via derivatisation with arylnitro labels", *Mater. Chem.*, **17** (2007) 3515–3524.
13. B. Šljukić, R. Baron, R.G. Compton, "Electrochemical determination of oxalate at pyrolytic graphite electrodes", *Electroanalysis*, **19** [9] (2007) 918–922.
14. X. Xu, S. Jiang, Z. Hu, S. Liu, X. Xu, S. Jiang, Z. Hu, S. Liu, "Nitrogen-doped carbon nanotubes: high electrocatalytic activity toward the oxidation of hydrogen peroxide and its application for biosensing", *ACS Nano*, **4** (2010) 4292–4298.
15. G. Ćirić-Marjanović, "Polyaniline nanostructures", p. 98 in: *Nano-structured Conductive Polymers*, Chapter 2. Ed. A. Eftekhari Wiley, London, 2010.
16. A. Janošević Ležaić, D. Bajuk-Bogdanović, M. Radoičić, V.M. Mirsky, G. Ćirić-Marjanović, "Influence of synthetic conditions on the structure and electrical properties of nanofibrous polyanilines and their nanofibrous carbonized forms", *Synthetic Met.*, **214** (2016) 35–44.
17. S. Mentus, G. Ćirić–Marjanović, M. Trchová, J. Stejskal, "Conducting carbonized polyaniline nan-

otubes", *Nanotech.*, **20** (2009) 245601–245611.
18. J.J. Langer, S. Golczak, "Highly carbonized polyaniline micro- and nanotubes", *Polym. Degrad. Stab.*, **92** (2007) 330–334.
19. G. Ćirić-Marjanović, I. Pašti, S. Mentus, "One-dimensional nitrogen-containing carbon nanostructures", *Progress Mater. Sci.*, **69** (2015) 61–182.
20. D. Yuan, T. Zhou, S. Zhou, W. Zou, S. Mo, N. Xia, "Nitrogen-enriched carbon nanowires from the direct carbonization of polyaniline nanowires and its electrochemical properties", *Electrochem. Commun.*, **13** [3] (2011) 242–246.
21. K. Chizari, I. Janowska, M. Houllé, I. Florea, O. Ersen, T. Romero, P. Bernhardt, M.J. Ledoux, C. Pham-Huu, "Tuning of nitrogen-doped carbon nanotubes as catalyst support for liquid-phase reaction", *Appl. Catal. A: General*, **380** (2010) 72–80.
22. N. Gavrilov, M. Vujković, I. Pašti, G. Ćirić-Marjanović, S. Mentus, "Enhancement of electrocatalytic properties of carbonized polyaniline nanoparticles upon a hydrothermal treatment in alkaline medium", *Electrochim. Acta*, **56** (2011) 9197–9202.
23. N. Gavrilov, M. Dašić-Tomić, I. Pašti, G. Ćirić-Marjanović, S. Mentus, "Carbonized polyaniline nanotubes/nanosheets-supported Pt nanoparticles: Synthesis, characterization and electrocatalysis", *Mater. Lett.*, **65** (2011) 962–965.
24. A. Janošević, I. Pašti, N. Gavrilov, S. Mentus, G. Ćirić-Marjanović, J. Krstić, J. Stejskal, "Micro/mesoporous conducting carbonized polyaniline 5-sulfosalicylatenanorods/nanotubes: Synthesis, characterization and electrocatalysis", *Synthetic Met.*, **161** (2011) 2179–2184.
25. D.H. Lee, J.A. Lee, W.J. Lee, D.S. Choi, W.J. Lee, S.O. Kim, "Facile fabrication and derived from polyaniline", *Carbon*, **50** (2012) 3915–3927.
26. T. Tang, B.L. Allen, D.R. Kauffman, A. Star, "Electrocatalytic activity of nitrogen-doped carbon nanotube cups", *J. Am. Chem. Soc.*, **131** (2009) 13200–13201.
27. A.Z. Sadek, C. Zhang, Z. Hu, J.G. Partridge, D.G. McCulloch, W. Wlodarski, K. Kalantar-zadeh, "Uniformly dispersed Pt–Ni nanoparticles on nitrogen-doped carbon nanotubes for hydrogen sensing", *J. Phys. Chem. C*, **114** (2010) 238–242.
28. G. Ćirić-Marjanović, "Recent advances in polyaniline research: Polymerization mechanisms, structural aspects, properties and applications", *Synthetic Met.*, **177** (2013) 1–47.
29. D. Micić, B. Šljukić, Z. Zujović, J. Travas-Sejdić, G. Ćirić-Marjanović, "Electrocatalytic activity of carbonized nanostructured polyanilines for oxidation reactions: sensing of nitrite ions and ascorbic acid", *Electrochim. Acta*, **120** (2014) 147–158.
30. B. Šljukić, I. Stojković, N. Cvijetićanin, G. Ćirić-Marjanović, "Hydrogen peroxide sensing at MnO_2/carbonized nanostructured polyaniline electrode", *Russ. J. Phys. Chem. A*, **85** [13] (2011) 2406–2049.
31. M. Mališić, A. Janošević, B. Šljukić Paunković, I. Stojković, G. Ćirić-Marjanović, "Manganese dioxide/carbon composite electrodes for simultaneous electroanalytical determination of lead(ii) and cadmium(II)", *Electrochim. Acta*, **74** (2012) 158–164.
32. B. Šljukić, D. Micić, N. Cvjetićanin, G. Ćirić-Marjanović, "Nanostructured materials for Pb(II) and Cd(II) ions sensing: manganese oxohydroxide versus carbonized polyanilines", *J. Serb. Chem. Soc.*, **78** [11] (2013) 1717–1727.
33. A. Janošević, I. Pašti, N. Gavrilov, S. Mentus, J. Krstić, M. Mitrić, J. Travas-Sejdic, G. Ćirić-Marjanović, "Microporous conducting carbonized polyaniline nanorods: Synthesis, characterization and electrocatalytic properties", *Micropor. Mesopor. Mater.*, **152** (2012) 50–57.
34. N. Gavrilov, I.A. Pašti, M. Vujković, J. Travas-Sejdic, G. Ćirić-Marjanović, S.V. Mentus, "High-performance charge storage by N-containing nanostructuredcarbon derived from polyaniline", *Carbon*, **50** (2012) 3915–3927.
35. B. Šljukić, C.E. Banks, R.G. Compton, "Exploration of stable sonoelectrocatalysis for the electrochemical reduction of oxygen", *Electroanalysis*, **17** [12] (2005) 1025–1034.
36. R.N. Goyal, S. Chatterjee, A.R.S. Rana, "A comparison of edge- and basal-plane pyrolytic graphite electrodes towards the sensitive determination of hydrocortisone", *Talanta*, **83** (2010) 149–155.
37. A.N. Patel, S. Tan, T.S. Miller, J.V. Macpherson, P.R. Unwin, "Comparison and reappraisal of carbon electrodes for the voltammetric detection of dopamine", *Anal. Chem.*, **85** (2013) 11755–11764.
38. C. Canales, F. Varas-Concha, T.E. Mallouk, G. Ramírez, "Enhanced electrocatalytic hydrogen evolution reaction: Supramolecular assemblies of metalloporphyrins on glassy carbon electrodes", *App. Catal. B: Environ.*, **188** (2016) 169–176.
39. H. Gerischer, R. Mcintyre, D. Scherson, W. Storck, "Density of the electronic states of graphite: derivation from differential capacitance measurements", *J. Phys. Chem.*, **91** [7] (1987) 1930–1935.
40. H.V. Patten, K.E. Meadows, L.A. Hutton, J.G. Iacobini, D. Battistel, K. McKelvey, A.W. Colburn, M.E. Newton, J.V. Macpherson, P.R. Unwin, "Electrochemical mapping reveals direct correlation between heterogeneous electron-transfer kinetics and local density of states in diamond electrodes", *Angew. Chem. Int. Ed.*, **51** [28] (2012) 7002–7006.
41. R.L. McCreery, "Advanced carbon electrode materials for molecular electrochemistry", *Chem. Rev.*, **108** [7] (2008) 2646–2687.
42. F. Tuinstra, J.L. Koenig, "Raman spectrum of graphite", *J. Chem. Phys.*, **53** (1970) 1126.
43. F. Negri, C. Castiglioni, M. Tommasini, G. Zerbi, "A computational study of the Raman spectra of large polycyclic aromatic hydrocarbons: Toward molecu-

larly defined subunits of graphite", *J. Phys. Chem. A*, **106** (2002) 3306–3317.
44. J. Xu, Q. Chen, G.M. Swain, "Anthraquinone disulfonate electrochemistry: a comparison of glassy carbon, hydrogenated glassy carbon, highly oriented pyrolytic graphite, and diamond electrodes", *Anal. Chem.*, **70** (1998) 3146–3154.
45. C.M.A. Brett, A.M.O. Brett, *Electroanalysis*, Oxford Chemistry Primers No. 64, Oxford University Press, Oxford 1998.
46. K.R. Kneten, R.L. McCreery, "Effects of redox system structure on electron-transfer kinetics at ordered graphite and glassy carbon electrodes", *Anal. Chem.*, **64** [21] (1992) 2518–2524.
47. R.R. Moore, C.E. Banks, R.G. Compton, "Electrocatalytic detection of thiols using an edge plane pyrolytic graphite electrode", *Analyst*, **129** (2004) 755–758.
48. R.N. Goyal, S. Chatterjee, A.R.S. Rana, "A single-wall carbon nanotubes modified edge plane pyrolytic graphite sensor for determination of methylprednisolone in biological fluids", *Talanta*, **80** (2009) 586–592.
49. C.E. Banks, R.G. Compton, "Edge plane pyrolytic graphite electrodes in electroanalysis: An overview", *Anal. Sci.*, **21** (2005) 1263–1268.
50. D.S. Shishmarev, N.V. Rees, R.G. Compton, "Enhanced performance of edge-plane pyrolytic graphite (EPPG) electrodes over glassy carbon (GC) electrodes in the presence of surfactants: Application to the stripping voltammetry of copper", *Electroanalysis*, **22** (2010) 31–34.
51. R.T. Kachoosangi, C.E. Banks, R.G. Compton, "Simultaneous determination of uric acid and ascorbic acid using edge plane pyrolytic graphite electrodes", *Electroanalysis*, **18** (2006) 741–747.
52. C.M. Welch, C.E. Banks, S. Komorsky-Lovric, "Electroanalysis of trace manganese via cathodic stripping voltammetry: Exploration of edge plane pyrolytic graphite electrodes for environmental analysis", *Croat. Chem. Acta*, **79** (2006) 27–32.
53. F. Wantz, C.E. Banks, R.G. Compton, "Direct oxidation of ascorbic acid at an edge plane pyrolytic graphite electrode: A comparison of the electroanalytical response with other carbon electrodes", *Electroanalysis*, **17** (2005) 1529–1533.
54. F. Wantz, C.E. Banks, R.G. Compton, "Edge plane pyrolytic graphite electrodes for stripping voltammetry: a comparison with other carbon based electrodes", *Electroanalysis*, **17** (2005) 655–661.
55. A.N. Patel, K. McKelvey, P.R. Unwin, "Nanoscale electrochemical patterning reveals the active sites for catechol oxidation at graphite surfaces", *J. Am. Chem. Soc.*, **134** [50] (2012) 20246–20249.
56. A.N. Patel, S.Y. Tan, P.R. Unwin, "Epinephrine electro-oxidation highlights fast electrochemistry at the graphite basal surface", *Chem. Commun.*, **49** (2013) 8776–8778.
57. M.A. Edwards, P. Bertoncello, P.R. Unwin, "Slow diffusion reveals the intrinsic electrochemical activity of basal plane highly oriented pyrolytic graphite electrodes", *J. Phys. Chem. C*, **113** (2009) 9218–9223.
58. S.C.S. Lai, R.A. Lazenby, P.M. Kirkmana, P.R. Unwin, "Nucleation, aggregative growth and detachment of metal nanoparticles during electrodeposition at electrode surfaces", *Chem. Sci.*, **6** (2015) 1126–1138.
59. G. Zhang, A.S. Cuharuc, A.G. Güell, P.R. Unwin, "Electrochemistry at highly oriented pyrolytic graphite (HOPG): Lower limit for the kinetics of outer-sphere redox processes and general implications for electron transfer models", *Phys. Chem. Chem. Phys.*, **17** (2015) 11827–11838.
60. W.J. Royea, T.W. Hamann, B.S. Brunschwig, N.S. Lewis, "A comparison between interfacial electron-transfer rate constants at metallic and graphite electrodes", *Phys. Chem. B*, **110** (2006) 19433–19442.